Pyrazine-2-carboxylate copper(II) complexes

Alma Araujo Martinez,^a Christopher P. Landee,^b Diane A. Dickie^c and Mark M. Turnbull^a,
^a Carlson School of Chemistry and Biochemistry, Clark University, 950 Main Street,
Worcester, MA 01610, USA. E-mail: mturnbull@clarku.edu

^b Department of Physics, Clark University, 950 Main Street, Worcester, MA 01610, USA

^c Department of Chemistry, University of Virginia, Charlottesville, VA 22904

Abstract

A pyrazine-2-carboxylate (pzCO₂) complex of copper(II) has been synthesized, studied structurally and magnetically, and compared with structurally similar compounds. The structure of [CuCl(pzCO₂)] (1) is reported and compared with the known structures of [Cu(pzCO₂)₂] (2) and [Cu(pzCO₂)₂(H₂O)₂] (3). Single-crystal X-ray diffraction measurements show that 1 crystallizes in the monoclinic space group Pc, with two crystallographically independent five-coordinate Cu(II) ions in a geometry close to square-pyramidal. It has a bilayer structure in the packing. Magnetic susceptibility data of 1 show that it exhibits weak ferromagnetic interactions (2J = 2.26(7) K). In contrast, magnetic susceptibility data of 2 and 3 show weak antiferromagnetic interactions.

Introduction

The magneto-structural relationships in transition metal complexes have been a topic of interest for decades. Cu(II) complexes have been studied extensively in this field, as they can behave as low-dimensional magnets in which the magnetic exchanges happen in one or two dimensions, such as chains, ladders and layers. A common ligand used in these complexes is pyrazine (pz). This nitrogenous heterocyclic ligand contains two nitrogen atoms in 1,4-positions in a six-membered aromatic ring, which gives the molecule the ability to coordinate to one metal ion on each of these sites, making it an exo-bidentate ligand. This results in compounds with M-pz-M links in their structures, which can pack as dimers, chains and two-dimensional or three-dimensional networks. The presence of these pz bridges between metal ions has also been found to be a magnetic super-exchange pathway. The aromaticity of pz

within the ring and delocalization of electrons towards the metal ions can mediate spin exchange interactions.² Families of compounds with pz and additional ancillary ligands have been characterized by their crystal structures and magnetic lattices.³ An example of these compounds is the well-studied [Cu(pz)(NO₃)₂], where it was found that the pz ligands provide the super-exchange pathway.⁴

The introduction of substituents onto the pz molecule, which can be electron-withdrawing or electron-donating groups, can create different interactions in coordination compounds and generate different packing motifs. The presence of coordinating substituents can also be useful for magnetic studies of how the exchange pathway is influenced by the steric restriction of the ligand. In particular, the addition of the carboxylate functional group has been of great interest in molecular magnetism. Carboxylates are electron withdrawing groups with respect to the pz ring, and they have a variety of coordination modes (shown in Figure 1). These coordination modes include monodentate, chelating and bridging, and the bridging mode in itself can have different geometries as the metal ions can be in *syn* or *anti*-conformations.

Figure 1. Common coordination modes of the carboxylate anion.

The ligand pyrazine-2-carboxylate (pzCO₂) can then combine the unique coordination properties of both the pz and carboxylate groups. The proximity of one nitrogen atom of the pz and the carboxylate group can make pzCO₂ a N,O,O'-bidentate chelating bridging ligand, which can form a five-membered chelate ring, as shown in Figure 2.⁹

$$\begin{array}{c|c}
O \\
\hline
O \\
N \\
\hline
N
\end{array}$$

Figure 2. Coordination of pzCO₂

There are 63 reported structures of coordination compounds of copper(II) with the pzCO₂ ligand that contain this five-membered chelate ring (CSD),¹⁰ and amongst the copper(II) compounds, only 14 contain chloride ions, most of them in combination with other ancillary ligands. Only one of these reported structures contains a chloride ion without halide bridges or additional ancillary ligands, but there are no magnetic susceptibility studies found in the literature. As part of our continuing studies of magneto-structural relations in Cu(II)-pyrazine compounds, we present the synthesis, crystal structure and magnetic properties of *cantena*[chlorido(μ₃-pyrazine-2-carboxylato)copper(II)] (1) and comparison of its magnetic properties to the known compounds [Cu(pzCO₂)₂] (2) and [Cu(pzCO₂)₂(H₂O)₂] (3).

Experimental

Materials and methods

Copper (II) chloride dihydrate and pyrazine-2-carboxylic acid (pz-2-CO₂H) were purchased from Aldrich Chemical and used as received. IR data were collected by ATR on a Perkin-Elmer Spectrum 100 infrared spectrometer. X-Ray powder diffraction data were collected using a Bruker AXS-D8 Focus X-ray Powder Diffractometer. Elemental Analyses were carried out by Marine Science Institute, University of California, Santa Barbara CA 93106.

Magnetic Data Collection

Magnetization data were collected using a Quantum Design MPMS-XL SQUID magnetometer. Finely ground crystals of each compound were packed into a #3 gelatin capsule and placed in a clear plastic straw for data collection. Data were collected as a function of field from 0 to 50 kOe at 1.8 K. As the field was reduced to 0 kOe several data points were recollected to check for hysteresis effects; no hysteresis was observed. The M(H) response was linear beyond 1kOe for all samples. Magnetization was also measured as a function of temperature from 1.8 to 310 K in a 1 kOe applied field. The data were corrected for the background signal (measured independently), the temperature independent paramagnetism of the Cu(II) ion and the diamagnetic contributions of the constituent atoms, estimated via Pascal's constants. All data were fit using the Hamiltonian $H = -2J\Sigma S_1 \cdot S_2$. One data point (215 K) showed a large error (12%) and was not included in fitting. Powder X-ray diffraction data were compared to the single crystal structure prior to magnetic data collection to ensure that the sample was the same phase as the single crystal structure (Figures S1-S3, Supp. Inf.). No impurities were detected.

Synthesis

catena-[Chlorido(μ₃-pyrazine-2-carboxylato)copper(II)] (1). CuCl₂·2H₂O (0.128 g, 1.03 mmol), pz-2-CO₂H (0.170 g, 0.99 mmol), and 20 mL of isopropanol were placed in a round bottom flask. The mixture was refluxed for 24 hours, during which the reaction mixture had a cloudy blue appearance. A turquoise precipitate was observed at the bottom of the flask and the supernate was clear and light blue. The precipitate was collected through vacuum filtration and washed with 5 mL of isopropanol. Its appearance consisted of small crystalline turquoise particles (0.153 g, 68.9%). IR (ν in cm⁻¹): 1659 s, 1639 s, 1604 w, 1463 w, 1425 w, 1362 s, 1282 w, 1188 m, 1162 m, 1064 m, 1049 m, 863 m, 786 m, 740 m. CHN calculated (found) for C₅H₄N₂O₂ClCu: C, 26.92 (26.52); H, 1.81 (2.02); N, 12.56 (12.46). Crystals suitable for single crystal X-ray diffraction were grown by slow evaporation of the filtrate in air at room temperature. IR data and comparison of the calculated and experimental powder patterns (see SI Figure S1) confirm that the initial ppt. and single crystals are the same phase.

X-ray Structure Analysis

Data for 1 were collected with ϕ and ω scans on a Bruker D8 Venture PhotonIII diffractometer equipped with an an Incoatec IµS 3.0 micro-focus sealed X-ray tube (Mo K α , λ = 0.71073 Å) and a HELIOS double bounce multilayer mirror monochromator using Bruker Instrument Service v.6.2.15 software within the APEX4 software suite. Cell parameters were refined using SAINT V8.40B, ¹² and absorption corrections were made with SADABS 2016/2. ¹³ The crystal structure for 1 was solved through direct methods for the primary atom sites using the SHELXS-15 program, ¹⁴ and the difference Fourier map for secondary atom sites. It was refined via least-squares analysis as a two-component inversion twin using SHELXL-2018. ¹⁵ Nonhydrogen atoms were refined anisotropically. All hydrogen atoms were placed in calculated positions and refined via a riding model using fixed isotropic thermal parameters.

Table 1. X-ray data collection and refinement parameters for 1

Empirical formula	C5H3ClCuN2O2	
Formula weight (g/mol)	222.08	
Temp (K)	100(2)	
Wavelength (Å)	0.71073	
Space group	Monoclinic, Pc	
a (Å)	6.9772(5)	
b (Å)	10.4580(7)	
c (Å)	9.6689(6)	
α (°)	90	
β (°)	106.613(2)	
γ (°)	90	
Volume (Å)	676.07(8)	
Z	4	
Density (calculated)	2.182	
Absorption coefficient	3.563	
F(000)	436	
Crystal size	0.025 x 0.045 x	
mm ³	0.107 mm^3	
θ range for data collection (°)	2.937-28.321	
Index ranges	-9≤ h ≤9	
	-13 ≤ k≤ 13	
	-12 ≤1 ≤ 12	
Reflections collected	3320	

Independent reflections	3154
Absorption correction	Multi-scan
Max-min trans.	0.6027 and 0.7457
Refinement method	Fsqd
Data / restraints / parameters	3320 / 200 / 2
Goodness-of-fit on F^2	1.075
Final R indices [I>2 σ (I)]	0.0409
R indices (all data)	0.0440
Largest diff. Peak and hole	1.268 and -0.812
Flack parameter	0.15(2)

1.1 Crystal Structure Analysis

Reaction of copper(II) chloride dihydrate with pzCO₂H in isopropanol at reflux gave 1, which crystallized in the monoclinic space group *P*c with 4 formula units in the unit cell and two crystallographically independent Cu(II) ions. Selected bond lengths and angles are given in Table 2, and the asymmetric unit is shown in Figure 3. For atoms in the N11 ligand, adding 10 to the atom number results in the equivalent atom in the N21 ligand.

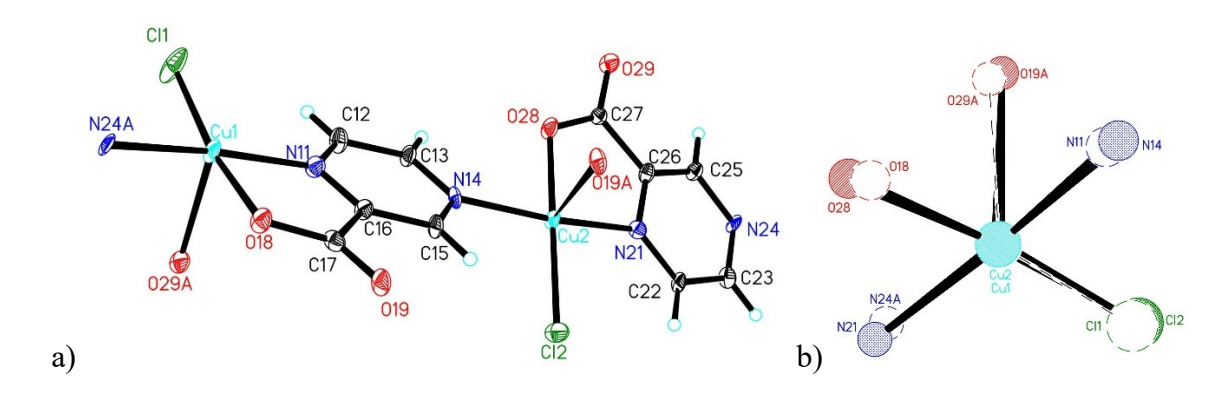


Figure 3.a) Thermal ellipsoid plot of the coordination environment of **1** showing 50% probability ellipsoids. Hydrogen atoms are shown as spheres of arbitrary size. Symmetry transformations used to generate equivalent atoms: N24A: -1+x, y, 1+z; O29A: x, y, 1+z; O19A/O29A: x, 1-y, -0.5+z. b) Fitted overlay of the two Cu-coordination spheres.

As shown in Figure 3, both Cu1 and Cu2 are five-coordinate. Each copper ion is coordinated to a chloride ion, two nitrogen atoms and two oxygen atoms. The nitrogen atom proximal to the carboxylate group (N11, N21) and one of the oxygen atoms of the carboxylate group (O18, O28) form a five-membered chelate ring with the adjacent carbon atoms and the copper ion.

The nitrogen atom distal to the carboxylate group (N14, N24) bridges the Cu(pzCO₂) units. The oxygen in the axial position (O29A, O19A) belongs to a pzCO₂ ligand in a neighboring molecular unit. Cu1 has a τ value of 0.0083 and Cu2 has a τ of 0.11, ¹⁶ indicating that both are very close to a square pyramidal geometry, with Cu2 slightly more distorted than Cu1. The similarities between the two coordination spheres is shown in Figure 3b. The Cu-O bond lengths for the axial oxygen atom, 2.336(4) and 2.409(5) Å, are longer than those for the equatorial oxygen atoms, 1.973(5) Å and 1.956(5) Å, as expected due to Jahn-Teller effects. In similar copper(II) and pzCO₂ complexes containing the 5-membered chelate ring and with a bridging carboxylate ion, the Cu-O(axial) bond is also longer than the Cu-O(equatorial) bond. Compounds [CuCl(pzCO₂)(H₂O)] and [Cu(N₃)(pzCO₂)(H₂O)] have Cu-O(axial) lengths of 2.213 Å and 2.244 Å respectively, while their Cu-O(equatorial) lengths are 1.975 Å and 1.973 Å respectively.¹⁷

In 1, each pzCO₂ ring is virtually planar within itself, as expected; their mean planes are 0.0059 Å and 0.0062 Å for the N11 and N21 rings respectively. The angle formed between the mean planes of the N11 and N21 rings is 147.2°, which indicates that the Cu1 and Cu2 coordination planes are twisted from each other. The five-membered chelate rings described previously are also relatively planar within themselves. These have mean plane deviations of 0.0093 Å and 0.0178 Å for the Cu1 and the Cu2-containing rings respectively. These five-membered rings are also nearly planar to the pzCO₂ ring they are fused to. The angle between the N11 ring and the Cu1 adjacent ring is 1.4° and that between the N21 ring and the Cu2 adjacent ring is 3.8°.

Table 2. Selected bonds [Å] and angles [°] for 1

Bond lengths (Å)			
Cu1-Cl1	2.235(2)	Cu2-Cl2	2.217(2)
Cu1-N11	2.016(9)	Cu2-N21	2.025(8)
Cu1-O18	1.973(5)	Cu2-O28	1.956(5)
Cu1-N24a (#1)	2.039(7)	Cu2-N14	2.010(8)
Cu1-O29a (#2)	2.336(4)	Cu2-O19a (#3)	2.409(5)
Bond angles (°)			
O18-Cu1-N24a (#1)	88.1(2)	O28-Cu2-N14	88.6(2)

N24a-Cu1-Cl1	94.6(2)	N14-Cu2-Cl2	94.2(2)
Cl1-Cu1-N11	94.8(2)	C12-Cu2-N21	94.8(2)
N11-Cu1-O18	82.2(3)	N21-Cu2-O28	82.0(2)
N11-Cu1-N24a (#1)	170.3(3)	N21-Cu2-N14	168.2(3)
O18-Cu1-Cl1	170.8(2)	O28-Cu2-Cl2	175.0(2)
O18-Cu1-O29a (#2)	87.8(2)	O28-Cu2-O19a (#3)	89.6(2)
N24a-Cu1-O29a (#2)	96.4(2)	N14-Cu2-O19a (#3)	81.9(2)
C11-Cu1-O29a (#2)	100.6(1)	C12-Cu2-O19a (#3)	95.0(1)
N11-Cu1-O29a (#2)	84.3(2)	N21-Cu2-O19a (#3)	105.0(2)

Symmetry transformations used to generate equivalent atoms: (#1) -1+x, y, 1+z (#2) x, y, 1+z (#3) x, 1-y, -0.5+z

As shown in Figure 4, 1 packs as a bilayer. The compound is first arranged into layers that form along the ac-plane (Figure 4a). This layer forms due to the different bridging modes of the pzCO2 ligand. The bridging through the nitrogen atoms of the pz ring allows for the formation of a chain along the c-axis. The bridging through the oxygen atoms in the axial positions occurs along the b-axis. The combination of these bridges creates the layer along the ac-plane. Within the same layer, there is the formation of loops involving four copper ions, which can be observed at the center of the unit cell in Figure 4b. Three of these copper ions are connected through carboxylate groups and the remaining one is bridged through a pz. The carboxylate groups which coordinate to the copper ions in the axial position do not bridge beyond the formation of these loops, limiting the extent of each individual layer. These layers then stack parallel to the b-axis. The chloride ions, shown in green in the figure, partially fill the space between these layers. The shortest Cu-O distance between layers is 5.051 Å and the shortest Cu-Cl distance between layers is 4.312(2) Å, supporting the isolation of the layers.

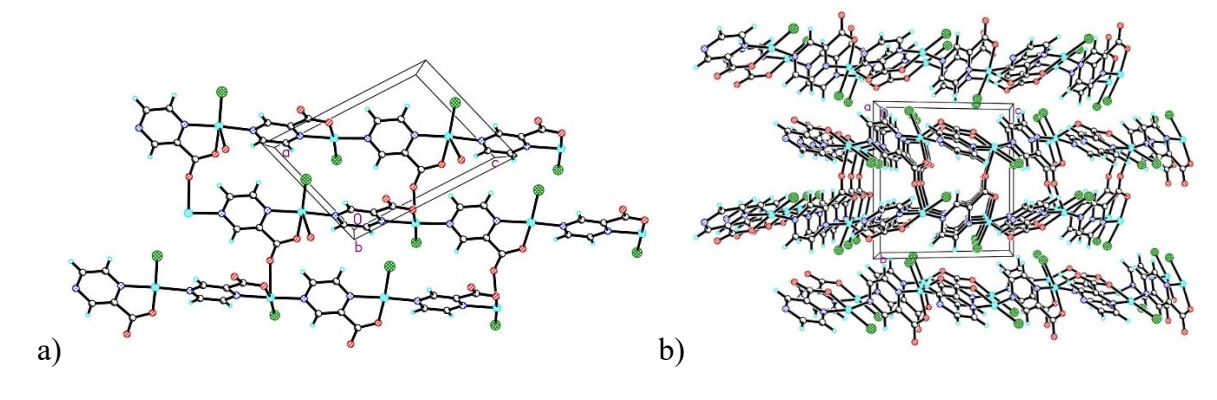


Figure 4. Packing diagrams of 1 a) showing a single layer of the bilayer, viewed parallel to the b-axis, b) showing the isolation of the bilayers viewed parallel to the a-axis.

Discussion

Initial attempts to synthesize 1 in solution resulted in copper compounds without chloride ions in their structure. Reactions of equimolar amounts of CuCl₂·2H₂O and pz-2CO₂H carried out in a 1:1 mixture of methanol and water resulted in a mixture of blue plate-shaped crystals, and turquoise prism-shaped crystals. The blue crystals, 2, were identified through their XRD powder pattern as [Cu(pzCO₂)₂]¹⁸ and the turquoise crystals, 3, were identified through their XRD powder pattern as Cu(pzCO₂)₂(H₂O)₂] (see SI figures S2 and S3).¹⁸ Changing the ratio of the solvents resulted in obtaining either compound 2 (more methanol) or 3 (more water).

A room temperature crystal structure of compound 1 has been reported, which was refined with a final R₁ value of 0.0942.¹⁹ The authors reported that the synthesis of the compound was carried out in an autoclave at 120°C for 48 hours by the reaction of CuCl₂·2H₂O with a compound containing a large heterocyclic structure, which generated pz-2CO₂H through *in situ* hydrolysis.¹⁹ To optimize our reaction conditions, a 24-hour reflux reaction was set-up with equimolar amounts of CuCl₂·2H₂O and pz-2CO₂H in 1-propanol, 1-butanol, ^tbutanol and isopropanol. The latter resulted in crystals of 1. Other reaction conditions yielded turquoise flake-like particles with an XRD powder pattern suggesting the presence of amorphous material in the product.

Magnetic Data

Field dependent magnetic data for 1 at 1.8 K display a downward curvature as shown in Figure 5. Hysteresis was not observed and M is linear from 0 to 5000 Oe (R^2 of 0.9955). Compound 1 reached a maximum of 5840 emu/mol at 50 kOe, which is in good agreement with the expected value for a Cu(II) complex of \sim 5800 emu mol⁻¹ for g slightly greater than 2.00, indicating that the moment is nearly saturated.

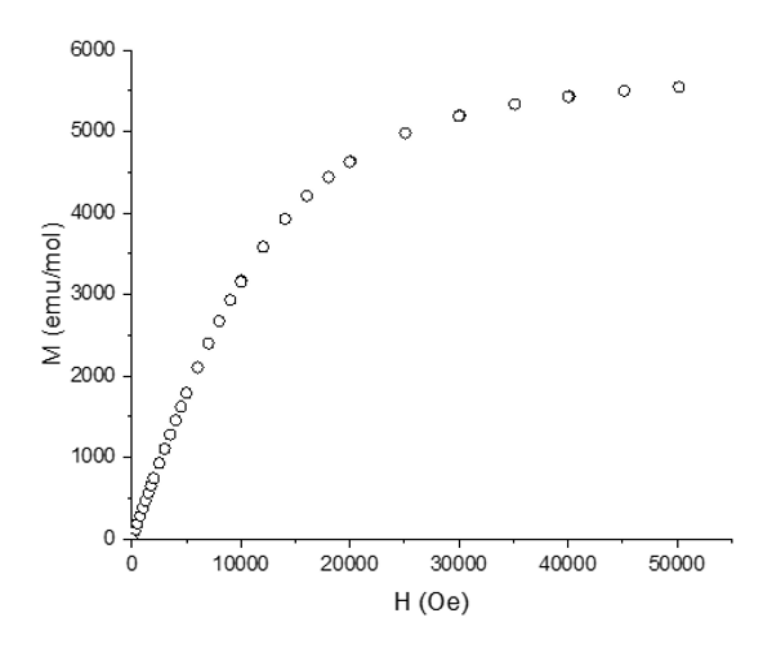


Figure 5. M(H) for **1** at 1.8 K.

The magnetic susceptibility as a function of temperature was measured from 1.8 K to 310 K in a 1 kOe field. $\chi(T)$ and $1/\chi(T)$ are shown in Figure 6. $\chi(T)$ increases steadily as temperature decreases without any local maximum. The $1/\chi(T)$ data were fit to the Curie-Weiss model,²⁰ resulting in a Curie constant (CC) of 0.432(1) emu-K/mol-Oe and a Weiss constant $\theta = 0.3(1)$ K. The small absolute value and positive sign of the Weiss constant are indicative of weak ferromagnetic interactions. The $\chi T(T)$ data, shown in Figure 7, also indicate that 1 has weak ferromagnetic interactions; the χT value rises with decreasing temperature to approximately 0.67 emu-K/Oe-mol at 1.8 K.

Given that 1 creates a chain of copper ions through pz and carboxylate bridges, the data were then modeled as 1D ferromagnetic chains with a Curie-Weiss correction for inter-chain interactions. The fitting parameters are shown in Table 3. The resulting Curie constants are in good agreement with the Curie-Weiss fit. The obtained exchange constants from both fits confirm the weak ferromagnetic interactions of the compound. The very small Curie-Weiss corrections (θ) indicate there is no significant interchain interaction.

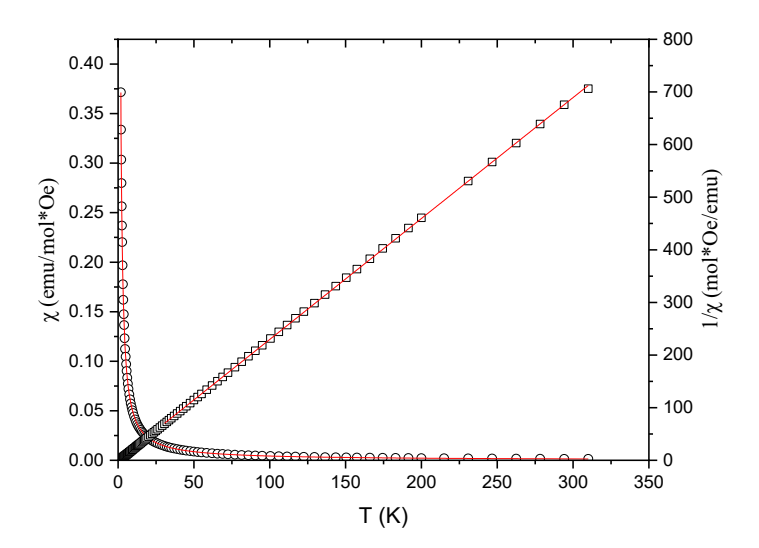


Figure 6. Magnetic susceptibility of **1** with $\chi(T)$ (open circles) and $1/\chi(T)$ (open squares). The fit to the 1D FM chain for $\chi(T)$ and the Curie-Weiss model for $1/\chi(T)$ are shown as solid lines.

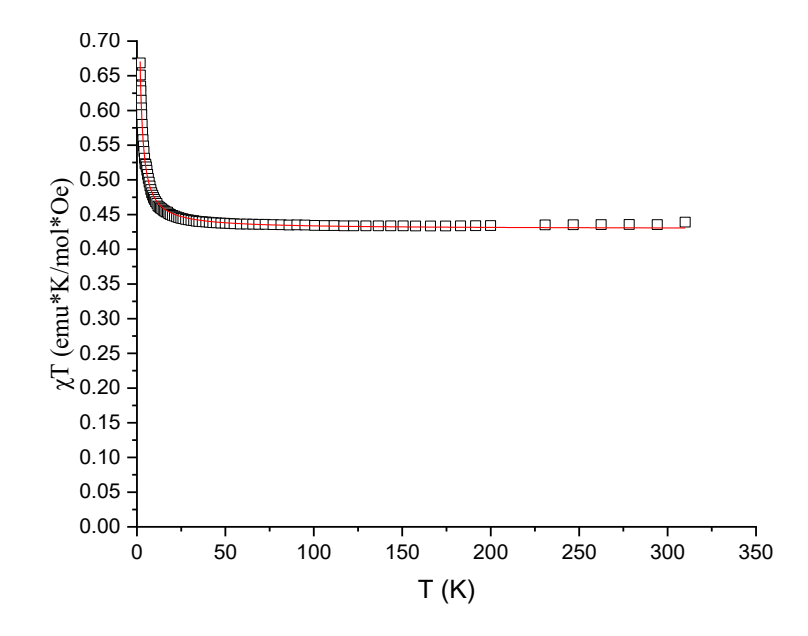


Figure 7. χ T(T) plot of **1**. The fit to the 1D-ferromagnetic model is shown as the solid line.

Table 3. Summary table of the magnetic data fit parameters for 1

Dataset	CC (emu- K/mol-Oe)	2J (K)	θ (K)
χ	0.426(1)	2.26(7)	-0.01(1)

γT	0.429(1)	1.95(7)	-0.06(2)
ι Λ *	0.127(1)	1.75(1)	0.00(2)

Although magnetic studies on transition metal complexes of pzCO₂ are scarce, there has been a great deal of research done on magneto-structural correlations of pz-bridged transition metal complexes. It is well known that pz can act as an antiferromagnetic exchange pathway in transition metal coordination complexes. Most of the known one-dimensional copper(II) compounds with substituted and unsubstituted pz ligands have AFM interactions.²¹ Therefore, the magnetic interactions of 1 do not seem to be explained via a superexchange pathway through the pz ring of the pzCO₂ ligand.

Watanabe and co-workers attempted the preparation of pyrazine-bridged Cu(II) compounds with FM exchange through designs intended to create axial-equatorial bridges between the ions, a known method for inducing FM exchange. 22 Three such compounds were prepared, but all showed negligible or AFM exchange. A compound similar to 1, [Cu(pzdc)] HCl, (pzdc=2,3pyrazinedicarboxylate), was reported to have weak FM interactions, and the authors attributed this to the orientation of the pz rings in the structure. However, the Cu(II) ions are also bridged by the carboxylate groups in the structure. The bridges link axial and equatorial positions on the Cu(II) ions. Carboxylate bridged ions have demonstrated ferromagnetic exchange in several instances. Klein et al. reported weak ferromagnetic exchange in Cu(pzCO₂)₂ (2) propagated via bridging carboxylates in the pzCO₂¹ ligand. They also reported weak ferromagnetic exchange in the hydrated analogue Cu(pzCO₂)₂(H₂O)₂ (3), but proposed that exchange in that complex was mediated by hydrogen bonding (neither pyrazine nor carboxylate bridges are present). Ferromagnetic exchange through carboxylate bridges have also been reported in carboxyl-substituted amino-alkylpyridine complexes²³ and in carboxylate bridged pyridyl-substituted amino acid complexes of Cu(II).²⁴ The carboxylate bridges in 1 link equatorial and axial sites between the Cu(II) ions and suggest that this is the most likely superexchange pathway in agreement with the observed FM exchange. The fitting results presented represent an averaging of the ferromagnetic contributions from the carboxylate bridges and the antiferromagnetic contributions from the pyrazine bridges. sophisticated model will be required to deconvolute the individual contributions.

Having prepared compounds 2 and 3, we were interested to reevaluate their magnetic properties. Magnetic susceptibility data of 2 and 3 were collected to compare with reported values and with the parameters obtained for 1. Klein and colleagues collected magnetic data in an atomic force magnetometer in the temperature range of 6 K - 300 K. They reported both compounds to have weak FM interactions, as indicated through Weiss constants of $\theta = 0.59$ K and $\theta = 0.30$ K and exchange constants 2J = 0.60 K and 2J = 0.33 K, for 2 and 3 respectively. They used a 1D-chain model for fitting both compounds; 2 is a structural 1D-chain linked through the pzCO₂ carboxylate groups and 3 is a linear chain linked through hydrogen-bonding. The results obtained suggest that the hydrogen-bonded chain compound has somewhat weaker interactions in comparison to the carboxylate bridged chain. Klein and colleagues indicated that it would be necessary to conduct these experiments at lower temperatures to confirm their findings because of the very weak interactions. The carboxylate is a superiment of the very weak interactions.

Magnetic susceptibilities as a function of temperature of both 2 and 3 were measured from 1.8 K to 310 K in a 1 kOe field. $\chi(T)$ and $1/\chi(T)$ of 2 are shown in Figure 8. $\chi(T)$ increases steadily as temperature decreases. The $1/\chi(T)$ data were fit to the Curie-Weiss model (solid line in Figure 8), resulting in a Curie constant of 0.426(1) emu-K/mol-Oe and $\theta = -0.12$ (3) K. The negative Weiss constant is indicative of weak AFM interactions.

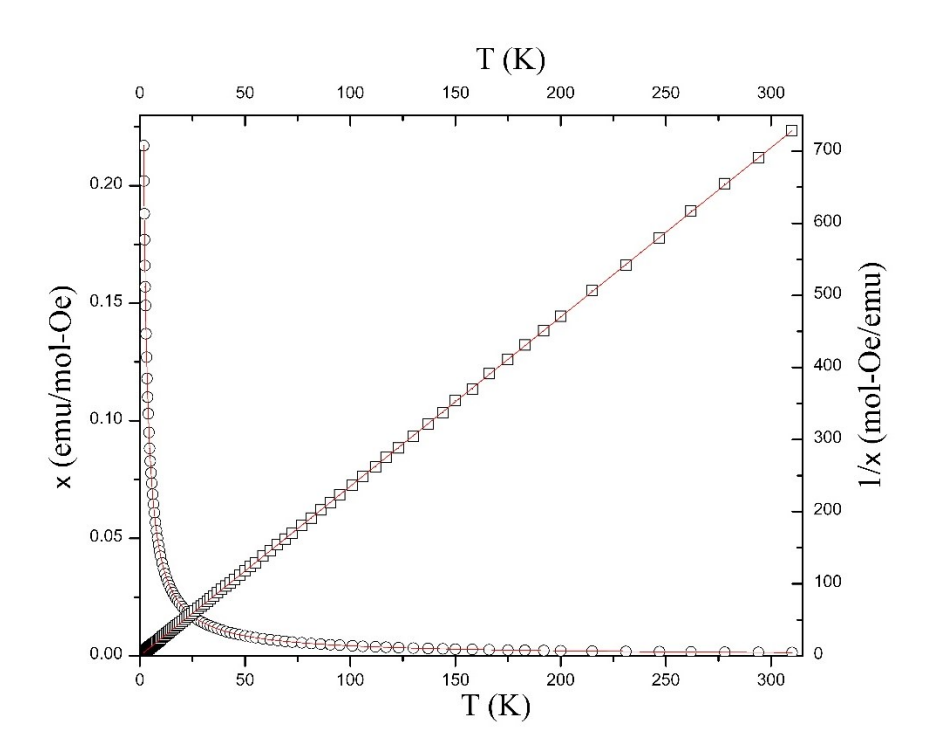


Figure 8. Magnetic susceptibility of 2 with $\chi(T)$ (open circles) and $1/\chi(T)$ (open squares). The fit to the AFM chain for $\chi(T)$ and the Curie-Weiss fit for $1/\chi(T)$ are shown as solid lines.

The AFM chain model was used to fit the $\chi(T)$ and $\chi T(T)$ data. The $\chi(T)$ data were fit resulting in CC = 0.425(1) emu-K/mol-Oe and 2J = -0.28(1) K. The $\chi T(T)$ graph (Figure S4) shows the characteristic downward curvature at low temperatures, indicative of AFM interactions. The fit of the data resulted in C = 0.444(1) emu-K/mol-Oe and 2J = -0.28(1) K.

The $\chi(T)$ and $1/\chi(T)$ data of **3** are shown in Figure 9. χ again increases steadily as temperature decreases. A Curie-Weiss fit to the $1/\chi$ data resulted in CC = 0.411(1) emu-K/mol-Oe and θ = -0.8(2) K. The $\chi T(T)$ graph in Figure S3 appears to be almost linear throughout the whole temperature range, although it shows a minimal decrease as temperature reaches 1.8 K. Considering **3** is a hydrogen-bonded chain, the $\chi(T)$ and $\chi T(T)$ data were also fit to an AFM chain model. The fit of $\chi(T)$ resulted in CC = 0.418(1) emu-K/mol-Oe and 2J = -0.007(7) K (zero within the experimental error). The fit of the $\chi T(T)$ data gave CC = 0.424 emu-K/mol-Oe and 2J = -0.092(8) K (again, nearly zero).

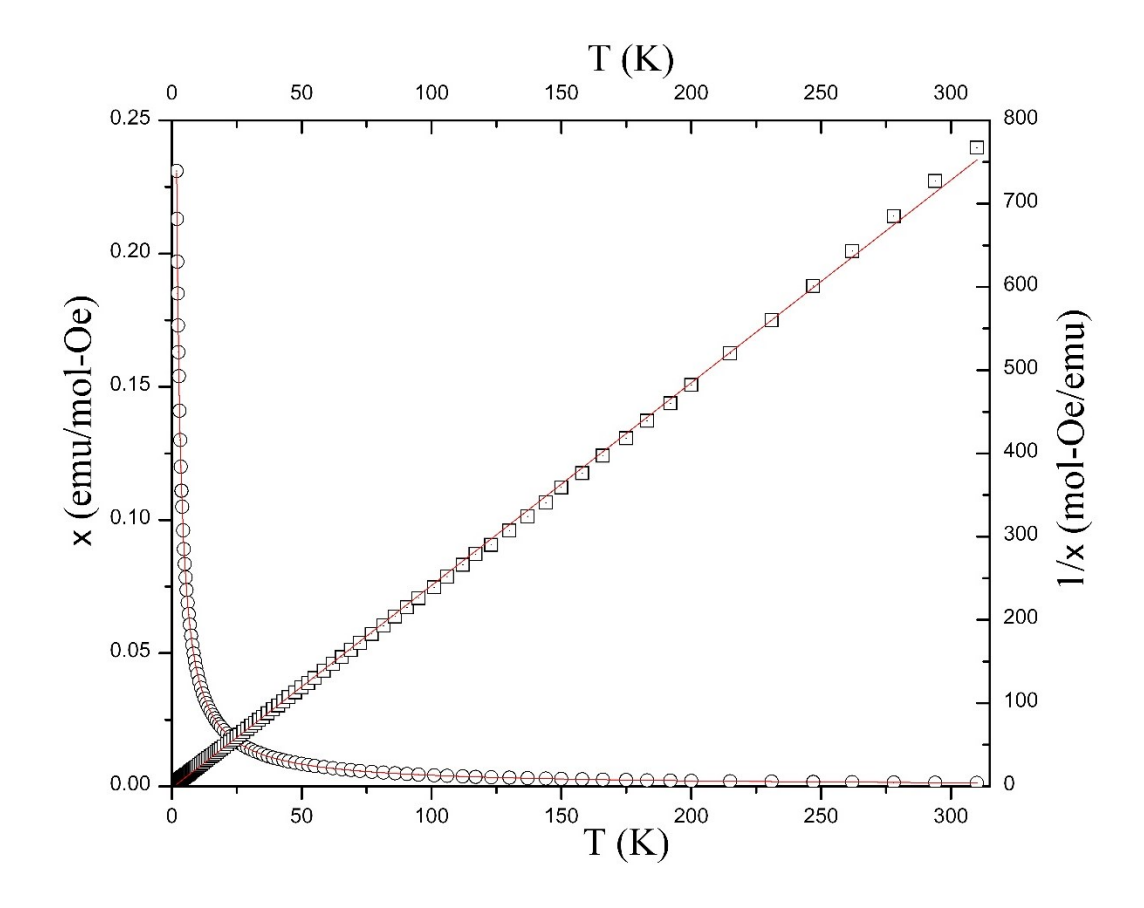


Figure 9. Magnetic susceptibility of **3** with $\chi(T)$ (open circles) and $1/\chi(T)$ (open squares). The fit to the 1D-AFM for $\chi(T)$ and the Curie-Weiss law for $1/\chi(T)$ are shown as solid lines.

Table 4. Summary table of the magnetic data fit parameters for 2 and 3.

Dataset	CC (emu-K/mol-Oe)	2J (K)
2		
χ	0.425(1)	-0.28(1)
χТ	0.444(1)	-0.28(1)
3		
χ	0.418(1)	-0.007(7)
χТ	0.424(3)	-0.092(8)

The magnetic data analysis for 2 and 3 reveal that these compounds have much weaker magnetic interactions than 1, but their behavior is not in agreement with the prior literature

where both compounds were believed to be weakly ferromagnetic. The difference in analysis is likely due to the lower temperature measurements in this study (1.8 K as opposed to 6 K) which are critical in the case of vanishingly weak interactions. Compound 2 was treated as a carboxylate bridged structural chain for the magnetic data analysis. Individual units of this bispzCO₂ compound are arranged in close proximity to each other, where the Cu(II) ions have an oxygen atom from the carboxylate of an adjacent molecule in close proximity. This Cu-O(axial) contact in 2 is 2.723 Å, ¹⁸ which is considerably longer than that found in 1. Compound 3 has an extended hydrogen-bonded network throughout the lattice resulting from its two aqua ligands which prevent carboxylate bridging. This structural feature causes the Cu(II) ions to be even further apart with an increased number of atoms possibly mediating the exchange. However, our results suggest that there are no interactions measurable down to 1.8 K. In contrast, in 1 the Cu(II) ions are linked through the pz and carboxylate group as well, therefore exhibiting stronger magnetic interactions.

Conclusions

A copper(II) complex with the pzCO₂ was prepared through direct synthesis and studied via its X-ray crystal structure and variable field and temperature magnetization. Compound 1, [CuCl(pzCO₂)], was synthesized in high yield through reflux in isopropanol. In the process of devising a reproducible synthetic procedure for 1, compounds 2, [Cu(pzCO₂)₂], and 3, [Cu(pzCO₂)₂(H₂O)₂] were also obtained. Single crystal X-ray diffraction showed that 1 displays five-coordinate copper(II) ions with a nearly square pyramidal geometry. The ligand is N,O,O'-bidentate, chelating and bridging, resulting in the formation of layers along the *ac*-plane, which then are stacked along the *b*-axis, packing into a bilayer.

Magnetic susceptibility data of 1, 2 and 3 were collected and interpreted. Compound 1 was found to have weak FM interactions, and the data were fit to the 1D FM chain with a Curie-Weiss correction. In contrast to 1, compounds 2 and 3 were found to have extremely weak AFM interactions, as evidenced through their zero Weiss constants and negligibly small exchange constants obtained through the AFM chain model. This is in contrast to the literature which reported very weak FM interactions for the compounds, but the new data was obtained to lower temperature providing for improved interpretation.

Acknowledgements

AAM is grateful for support from an anonymous donor. We are grateful for funds from PCI Synthesis, part of SEQENS CDMO, toward the purchase of the D8 Focus diffractometer, from the National Science Foundation (IMR-0314773) for purchase of the MPMS SQUID magnetometer, and from the Kresge Foundation for both. Single crystal X-ray diffraction experiments for 1 were performed on a diffractometer at the University of Virginia funded by the NSF-MRI program (CHE-2018870).

Supplementary data

CCDC (1, 2201034) contains the supplementary crystallographic data for 1 and is available free of charge from The Cambridge Crystallographic Data Centre via www.ccdc.cam.ac.uk/structures.

References

- 11. R.L. Carlin, Magnetochemistry. Springer-Verlag, Berlin/Heidelberg: Germany, 1986.
- 12. SAINT V8.40B (Bruker Nano, Inc.), 2019.
- 13. L. Krause, R. Herbst-Irmer, G.M. Sheldrick, D. Stalke, D., SADABS-2016/2 Bruker AXS area detector scaling and absorption correction **2015**.

^{1.} C.P. Landee, M.M. Turnbull Eur. J. Inorg. Chem. 2251 (2013).

^{2.} M. Inoue, M. Kubo, Coord. Chem. Rev. 21, 1 (1976).

^{3.} W. Kaim Angew. Chem. 22, 171 (1983).

^{4.} A. Santoro, A.D. Mighell, C.W. Reimann, Acta. Crystallogr. B: 26, 979 (1970).

^{5.} F. Taghipour, M. Mirzaei, M. Acta Crystallogr., Sect. C: 75, 231 (2019).

^{6.} C.J. O'Connor, C.L. Klein, R.J. Majeste, L.M. Trefonas, *Inorg. Chem.*, 21, 64 (1982).

^{7.} J.M. Ellsworth, H.-C. zur Loye Dalton Trans. 5823 (2008).

^{8.} N.R. de Campos, M.A. Ribeiro, W.X.C Oliveira, D.O. Reis, H.O. Stumpf, A.C. Doriguetto, F.C. Machado, C.B. Pinheiro, F. Lloret, M. Julve, J. Cano, M.V. Marinho *Dalton Trans.*, **45**, 172 (2016).

^{9.} M.A.S. Goher, N.A. Al-Salem, F.A. Mautner, K.O. Klepp, *Polyhedron* 16, 825 (1997).

^{10.} I.J. Bruno, J.C. Cole, P.R. Edgington, M. Kessler, C.F. Macrae, P. McCabe, J. Pearson, R. Taylor, *Acta Cryst.*, **B58**, 389 (2002).

- 14. G.M. Sheldrick, G., Acta Crystallogr., Sect. A: 64, 112.(2008)
- 15. Sheldrick, G. M., Acta Crystallogr., Sect. C: 27, 3 (2015).
- 16. A.W. Addison, T.N. Rao, J. Reedijk, J. van Rijn, G.C. Verschoor *J. Chem. Soc., Dalton Trans.* 1349 (1984).
- 17. M.A.S. Goher, M.A.M. Abu-Youssef, F.A. Mautner, *Polyhedron* 17, 3305 (1998).
- 18. C.L. Klein, R.J. Majeste, L.M. Trefonas, C.J. O'Connor, C. J., *Inorg. Chem.*, **21**, 1891 (1982).
- 19. Z.-Z. Wen, X.-L. Wen, S.-L. Cai, S.-R. Zheng, J. Fan, W.-G. Zhang, *CrystEngComm* **15**, 5359 (2013).
- 20. C.P. Landee, M.M. Turnbull, J. Coord. Chem., 67, 375 (2014).
- 21. J.L. Manson, Q.-z. Huang, J.W. Lynn, H.-J. Koo, M.-H Whangbo, R. Bateman, T. Otsuka, N. Wada, D.N. Argyriou, J.S. Miller, *J. Am. Chem. Soc.*, **123**, 162 (2001).
- 22. Watanabe, R.; Shimada, T.; Koyama, N.; Ishida, T.; Kogane, T. *Polyhedron* **30**, 3165 (2011).
- 23. H. Arora, F. Lloret, R. Mukherjee Dalton Trans. 9759 (2009).
- 24. K.-Y. Choi, S.-Y. Park, Y.-M. Jeon, H. Ryu, Struct. Chem. 16, 649 (2005).